Mine Water Environ (2018) 37:625–635
DOI 10.1007/s10230-017-0486-9

TECHNICAL COMMUNICATION

New Karst Sinkhole Formation Mechanism Discovered in a Mine Dewatering Area in Hunan, China

Xiaozhen Jiang[1] · Mingtang Lei[1] · Yongli Gao[2]

Received: 20 December 2016 / Accepted: 28 August 2017 / Published online: 27 September 2017

Abstract The Meitanba Coal Mine in Hunan province, China, has experienced severe karst sinkhole hazards since 1982. Mine dewatering that began in 1955 has produced a groundwater cone of depression encompassing an area of 219.19 km^2 as of 2014. Most dewatering-induced sinkholes occurred on three occasions: at the beginning of dewatering, at times when groundwater level dropped beneath the bedrock surface, and at times when water inrushes occurred. Sinkholes would not be typically anticipated in the stabilized groundwater cone of depression. However, over the last decades, many sinkholes including a large one, 80 m in diameter and 30 m in depth, that occurred at a primary school in 2010 have formed in the dewatering zone, even though a series of treatments have been taken to prevent such karst hazards. To determine the dynamic mechanisms of the sinkhole formation in the dewatering zone, the Dachengqiao region was selected as a study site and high-frequency monitoring of groundwater–air pressures was performed in the underlying karst conduit system. The monitoring results showed very intense pressure changes in the dewatering zone with a maximum fluctuation of 54.72 m and a maximum instant fluctuation rate of 70.6 cm H_2O/min. The abrupt pressure changes are more likely caused by air blasting and soil collapse and can be a key factor triggering the sinkhole collapses.

Keywords Karst collapse · Groundwater cone of depression · Groundwater–air pressure · Air blasting · Mining

Introduction

The Meitanba Coal Mine, located in Ningxiang County of Hunan province, China, was infamous for frequent mine flooding by karst water. Coal mining began there in 1955 and currently encompasses 25 km^2 with 34 shafts. The mining elevation is −400 m below mean sea level. Persistent dewatering of the karst aquifer has resulted in a groundwater cone of depression over an area of 219.19 km^2, as measured in 2014. The average radius of influence was 16.7 km. Dachengqiao town, which is in the south of the groundwater cone of depression and approximately 2 km from the mine, has experienced 171 karst collapses since 1982. The collapses have damaged 3,202 houses, 0.28 km^2 of farmland, 0.06 km^2 of woodland, 580 m of irrigation canals, and 60 dams. They have also destroyed a bridge and dried up 44 reservoirs. The direct economic loss was estimated to be 64.5 million US dollars (Chen et al. 2010). In 2010, a large collapse, 80 m in diameter and 30 m in depth, occurred on the playground of the Fuquan Primary School and forced the relocation of the school and the town of Dachengqiao.

Sinkholes are often induced at the beginning of dewatering, at times when groundwater levels drop below the bedrock surface, and when water inrushes occur (Xiao et al. 2008). Such experience suggests that sinkhole occurrence would be rare at other times in the dewatering zone. Over the last decade, however, more and more sinkholes have

✉ Xiaozhen Jiang
jxz@karst.ac.cn

Mingtang Lei
lmt@karst.ac.cn

Yongli Gao
yongli.gao@utsa.edu

[1] Key Laboratory of Karst Collapse Prevention, Institute of Karst Geology, CAGS, Guilin, China

[2] Center for Water Research, Dept of Geological Sciences, University of Texas at San Antonio, San Antonio, USA

formed in the Dachengqiao area, even though a series of engineering measures commonly used in other karst areas to prevent and remediate sinkholes (i.e. installation of grout curtains, ventilation to release air pressure, and backfilling depressions with soil and rock and then covering them with reinforced concrete slabs) have been taken (Sowers 1996; Xiao et al. 2008; Zhou and Beck 2008). The effectiveness of these treatments was limited due to inadequate understanding of the formation mechanisms of the karst collapses in the dewatering zones (Hu and Wang 2007). Several technologies were used to analyze the mechanism of sinkhole formation in the Dachengqiao area, including groundwater–air dynamic monitoring of the groundwater–air pressures in the karst conduit system.

The Geological Setting

The Meitanba area is characterized with a hilly landform consisting of eroded karst features. The ground elevation varies from 60 to 150 m above mean sea level. Most slopes range from 10° to 25° with dense vegetation. Structurally, the Meitanba and Wumuchong synclines form a double-syncline system that contains coal seams. The Bantangchong normal fault passes the Dachengqiao area in the direction of NE-NEE (Fig. 1).

The town of Dachengqiao is located south of the Meitanba Mine. The rock formations in the Meitanba area consist of Cretaceous (K_{eb}) conglomerate and sandstone, Permian (P) limestone, and Carboniferous (C_{2h}) limestone, which is overlain by Quaternary deposits (Table 1).

The average annual rainfall in this area is 1434 mm, with rainfall concentrated in April through July. The maximum annual precipitation is 2001.7 mm, and the maximum monthly and daily precipitations are 566.4 mm and 158.9 mm, respectively.

The study site is within the mine's dewatering zone but is also the mine's groundwater recharge area. The groundwater currently flows from south to north. The Dachengqiao River is the main river flowing through Dachengqiao, with flow rates ranging from 0.47 to 25 m^3/s. Water level elevations in the river range between 62.87 and 67.5 m above mean sea level. The river has a close hydraulic connection to the Meitanba Mine's groundwater system and is one of the mine's recharge sources.

Monitoring Method

Groundwater–air dynamic monitoring technology, Brillouin optical time domain reflectometry (BOTDR, a distributed optical fiber sensing technology), and ground penetrating radar were used to establish a comprehensive karst collapse monitoring network to better understand the formation mechanism of karst collapses in the Dachengqiao dewatering area (Jiang et al. 2016). Fourteen water–air pressure monitoring wells were installed in July 2013 to collect data on groundwater–air pressures of the karst conduit system. High-precision water–air pressure transducers, pore-water pressure sensors, and a remote data logging system were installed. Data was logged every 5 to 10 min to reflect the potential rapid groundwater–air pressure changes.

Figure 2 shows some of the karst collapses and the placements of the monitoring wells. The monitoring wells were distributed in the recharge zone with the exception of monitoring points CK8 and YR3, which were outside of the dewatering area. One monitoring well was installed in the Quaternary overburden, and monitoring boreholes YR12 and ZK12 were for air pressure only.

Results Analysis

The study area belongs to the dewatering zone of the Meitanba Mine. The depth to groundwater is greater than 90 m in the dry season (Fig. 3). Karst is intensely developed in the K_{eb} calcareous conglomerate and thick P_{1q} limestone. An unconformity exists between P_{1q} and the overlying K_{eb} formations. The karstic aquifers, K_{eb} and P_{1q}, have a strong hydraulic connection. The characteristic parameters of the monitoring points are presented in Table 2. The groundwater–air pressure data were converted to groundwater depth or elevation so that we could compare the results at different monitoring points.

Groundwater Dynamics

The Quaternary deposits of the study area consist of clay near the river and rubble and silty clay and red-brown clay in the hills. The thickness of the clay layers range from 1 to 2 m and their depth is between 5 and 6 m. A field survey of hand-dug wells indicates that there is very limited groundwater at depths below this layer. Farmers' wells are mainly located in the hilly areas where there is only enough water to supply a household.

The depth to groundwater in the hand-dug wells ranges from 0.1 to 4.37 m. No engineering activities affects this groundwater, which responds rapidly to rainfall events. Groundwater level rose significantly in response to rains that lasted longer than 15 min and dropped almost as soon as the rains stopped. Such groundwater responses are typical for such geological structure, where the clay aquiclude is overlain by intensively weathered rubble and silty clay, which allows surface runoff to infiltrate rapidly.

Table 3 presents monitoring results of groundwater–air pressures in the karst conduit system within the dewatering

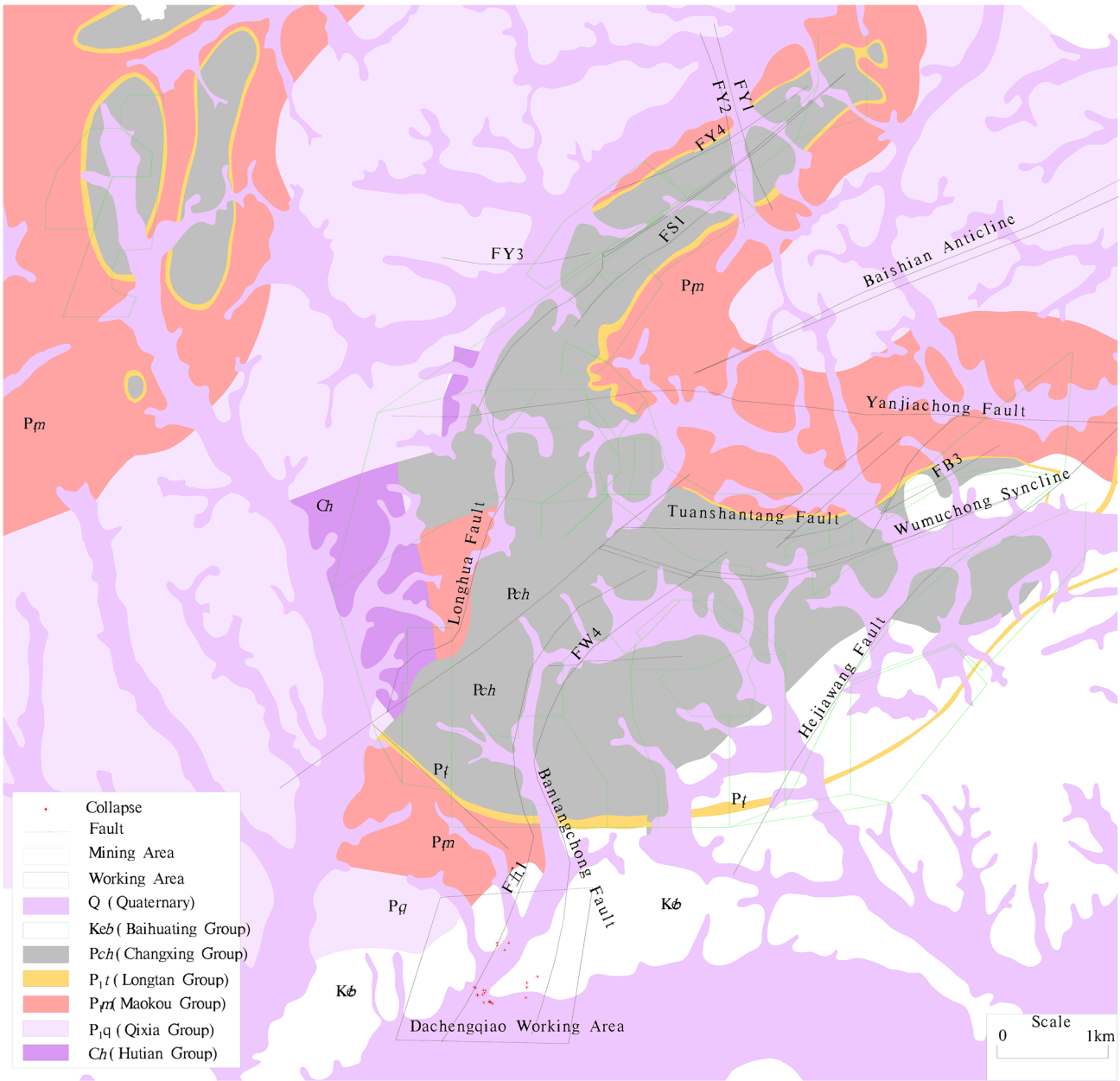

Fig. 1 Regional geological map of Meitanba area

zone. Karst groundwater elevations ranged between −19.1 and 72.5 m. Most monitoring points showed pressure changes >25 m, with the exceptions of YR5, ZK11, and YR6.

The K_{eb} and P_{1q} are the main karst aquifers in this area. The borehole data revealed bead-like cavities in those aquifers. At depths of 20–60 m, water flow was audible in boreholes CK7, ZKW1, and Oujia, indicating that the upper K_{eb} conglomerate aquifer water flows vertically to the underlying P_{1q} limestone aquifer. The direction of karst groundwater flow is from south (Dachengqiao) to north (the Meitanba coal mine pit). The groundwater fluctuation was caused by rainfall (Fig. 4) with a maximum of 54.72 m in CK7. The actual groundwater fluctuation was likely larger than 54.72 m because the depth of the groundwater level was usually less than 94 m where the sensor was installed. The change in YR6 was the smallest because the borehole did not reach to the karst conduit system at its completion depth of 63.58 m.

The abrupt changes related to variations of groundwater–air pressure were observed at monitoring points in the recharge zone, such as YR12, Oujia, YR1, YR2m and

Table 1 Summary of the strata in Meitanba area, *Ls* limestone, *Ss* sandstone, *cong* conglomerate

	Stratigraphic age	Code	Thickness (m)	Lithology
1	Quaternary	Q	3.5–30	Residual and alluvial silty clay, pebbly coarse sand, and sandy gravel
2	Baihuating group, Cretaceous	K_{eb}	0–480	The upper part contains purple red siltstone, glutenite, and argillaceous cementation. The middle is Ss and cong. with iron and argillaceous cementation. The lower part contains purple red conglomerate, where gravels are dominated by 8–20 cm in diameter Ls fragments with calcareous argillaceous cement
3	Changxing group, Permian	P_{ch}	30–400	Medium to thick-bedded aphanitic thick-bedded Ls, siliceous Ls and medium to thick-bedded aphanitic and fine bioclastic Ls
4	Longtan group, Permian	P_{lt}	6–38	Argillite, coal bed, claystone, sandy claystone
5	Maokou group, Permian	P_{lm}	300	Microcrystalline and fine crystalline thick-bedded Ls, argillaceous Ls
6	Qixia group, Permian	P_{lq}	>500	Siliceous limestone and limestone with a thickness of medium to thick-bedded, argillaceous limestone
7	Hutian Group, Carboniferous	C_{2h}	>200	Thick-bedded limestone in gray-white and light grey. Some parts contain chert nodules. It contains local light red dolomitic limestone

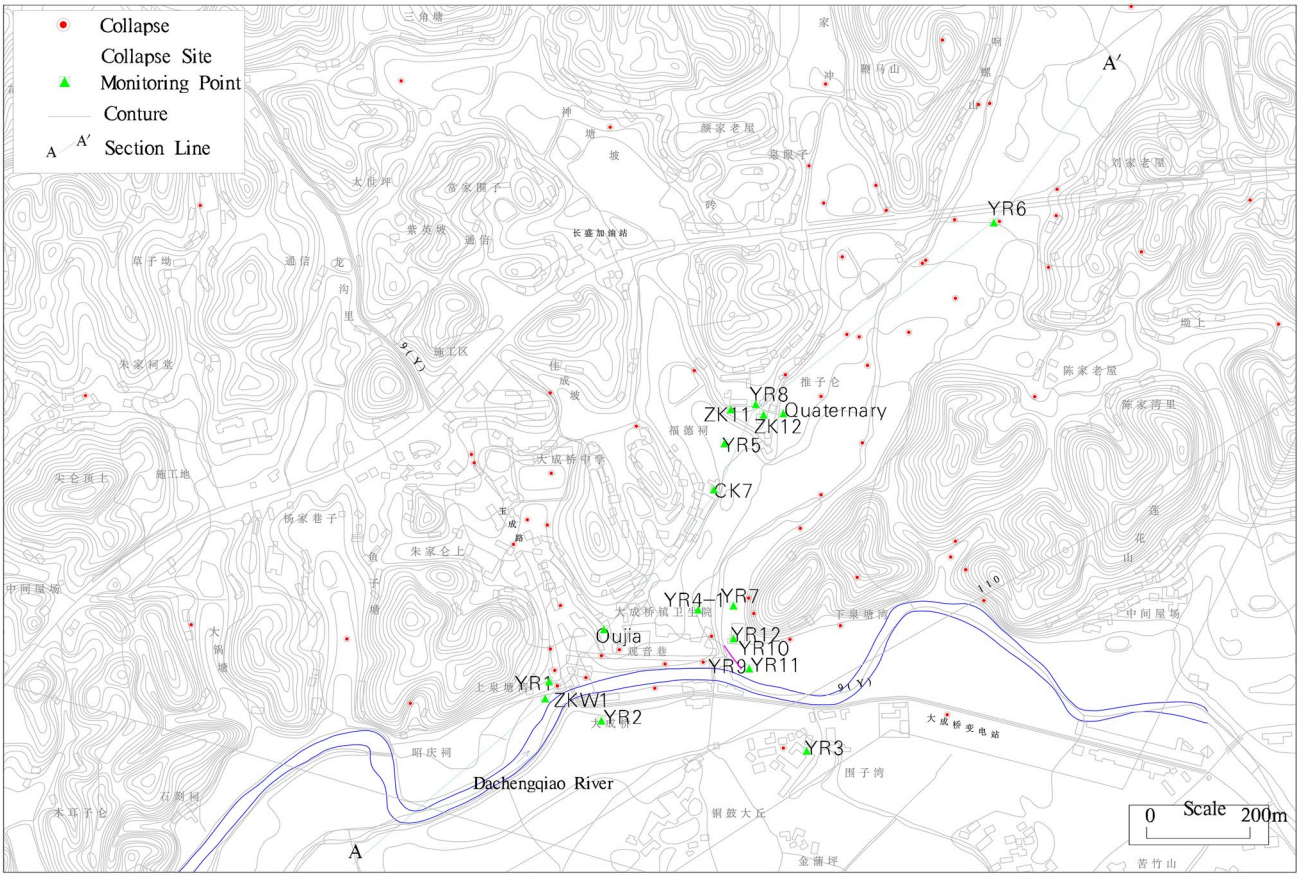

Fig. 2 The distribution of karst collapses and monitoring points in Dachengqiao

ZKW1, with the maximum of 70.6 cm H_2O/min. The most obvious changes occurred at monitoring points YR12 and Oujia.

Characterization of Abrupt Groundwater–Air Pressure Changes

The monitoring data show 251 abnormal changes at the monitoring points. The number of abrupt changes of groundwater–air pressure increases with rainfall intensity (Fig. 5).

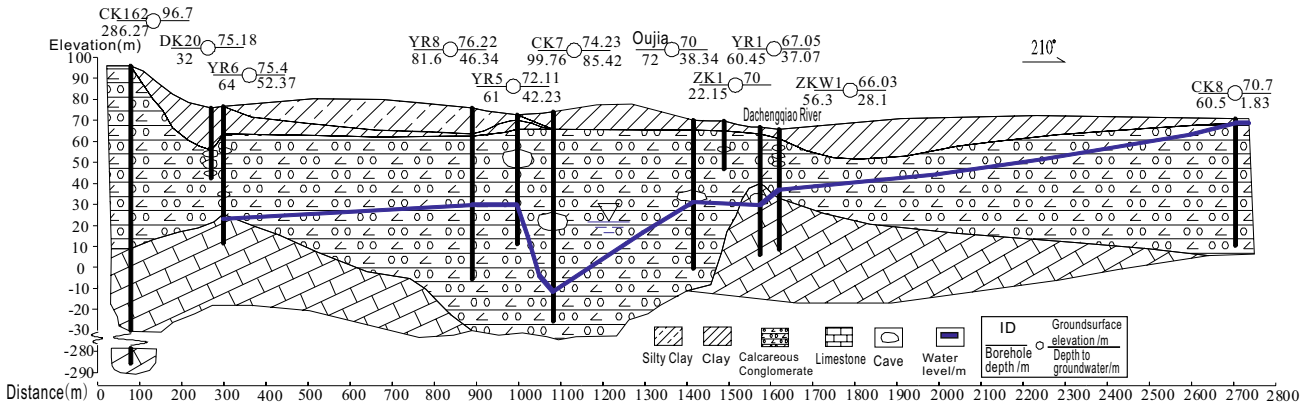

Fig. 3 The geological cross-section (groundwater levels measured 2 June 2014)

Table 2 Features of monitoring points (MPs); *GW* groundwater, *Quat* quaternary

MP	Borehole depth (m)	Depth to GW (m)	GW level (m)	Sensor depth (m)	Thickness of Quat. (m)	Thickness of K_{eb} (m)	Thickness of P_{1q} (m)
CK8	60.50	1.18	69.891	35.00	1.60	58.90	
CK7	99.76	46.00	46.845	94.00	7.80	91.96	
Oujia	72.00	38.45	31.515	65.85	4.80	67.20	
YR1	60.45	41.15	21.184	55.00	1.95	29.20	29.30
YR2	60.40	51.28	14.915	58.00	20.50	26.00	13.90
YR3	42.00	4.00	64.874	30.00	11.00	31.00	
YR4-1	98.85	16.40	50.325	90.00	9.40	89.45	
YR5	61.00	39.64	32.47	58.00	6.00	55.00	
YR6	63.58	51.90	23.657	60.00	11.50	37.40	15.10
YR7	40.40	5.66	60.809	37.00	8.40	32.00	
Quat	5.25	1.20	73.807	5.25			
ZKW1	56.30	34.23	32.236	34.45	4.20	23.90	28.20
YR12	6.00			3.98	4.00	2.00	
ZK12	80.70	58.96	16.057	5.00	8.10	72.60	

Table 3 Variation of groundwater–air pressures in dewatering karst area; *MP* monitoring point, *GW* groundwater, *min* minimum, *max* maximum

MP	Instant variation rate of GW (cm H_2O/min)	Min GW elevation (m)	Max GW elevation (m)	Depth of GW (m)	Variation range (m)
CK7	−5.8 to 26.7	−19.07	35.65	38.7–93.42	54.72
Oujia	−69 to 69	21.16	62.75	7.2–48.8	41.59
YR1	−25 to 70.6	21.25	68.02	−0.83 to 46	46.77
YR2	−20 to 66.4	11.86	63.66	2.53–54.3	51.8
YR4-1	−19 to 16.7	37.1	71	−3.87 to 29.6	33.9
YR5	−3.8 to 5	29.53	34.56	37.6–42.6	5.03
YR6	−21.5 to 2.78	22.97	23.96	51.6–52.6	0.99
YR7	−5.8 to 26.7	41.9	67.7	−1.24 to 24.54	25.8
ZKW1	−37.8 to 50.1	31.3	72.5	−6.1 to 35.2	41.2
ZK11	11.8	16.75	4.54	58.27–70.48	12.21

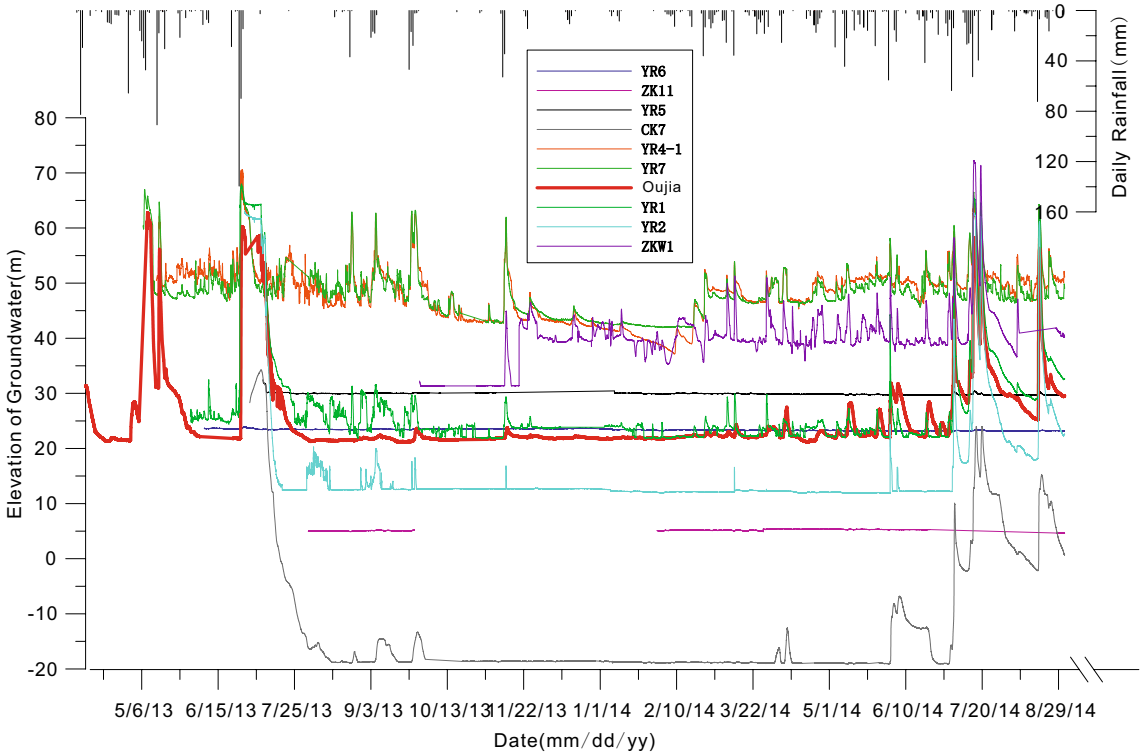

Fig. 4 The relationship between groundwater–air pressures and rainfall in the period from April 2013 to September 2014

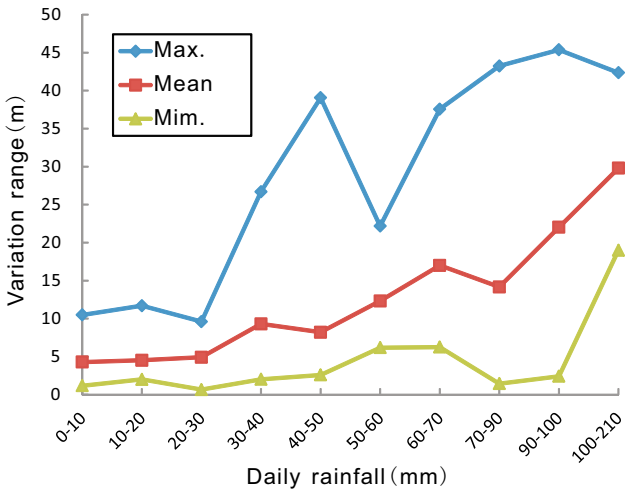

Fig. 5 The relationship between fluctuation of groundwater level and rainfall

Daily rainfalls of 30, 60, and 100 mm are three distinct points at which obvious groundwater level increases were observed. Detailed explanations are:

1. If the daily precipitation was less than 30 mm, the groundwater level did not rise significantly, with an average variation range of 4.6 m.
2. If the daily precipitation was between 30 and 60 mm, the groundwater level rose, and the maximum variation range increased rapidly. The average variation range also increased significantly, up to 10 m.
3. If the daily precipitation was between 60 and 100 mm, the groundwater level increased significantly and the average variation range was up to 17.7 m.
4. If the daily precipitation was more than 100 mm, the minimum variation was 19 m and the average variation range was up to 42.4 m.

Analysis of Factors Inducing Abrupt Pressure Changes

The number of sinkholes has been increasing annually in this study area although there are no longer any human activities in this dewatering area. Analysis of the abrupt pressure changes and in-situ investigation indicates that they may be caused by two factors, air blasting (Standing et al. 2013; Little 1984; He and Xu 1993) and soil/rock collapses. Both were observed frequently at some monitoring points.

Air Blasts

Air blasts in the karst conduit system within the dewatering area appears to be related to the amount of rainfall. When daily precipitation >60 mm, air blasts were observed

frequently in the dewatering area. This occurred because the karst groundwater level in this area is below the bedrock surface and the lag time of the groundwater level increase is ≈2 to 10 h after the rainfall. During heavy rains, a sealing layer was formed between the karst groundwater and the Quaternary overburden because of the low-lying land and recharge from the Dachengqiao River. As a result, the air between the Quaternary overburden and the karst conduit system was compressed and then blasted. Frequent air blasting was observed at three monitoring points, YR4-1, Oujia, and YR12, when the instant variation rate of the groundwater–air pressures was over 7 cm H_2O/min in the karst conduit system. Some notable examples are discussed below.

On June 26th, 2013, the groundwater elevation at YR4-1 rose rapidly during an extreme rainstorm. The maximum elevation of the groundwater–air pressure reached 70.5 m (higher than the ground elevation of 66.3 m) and then declined. This all occurred within ≈40 min, during which, the instant variation rate of groundwater–air pressure was up to −18 cm H_2O/min (Fig. 6). This phenomenon has occurred many times according to monitoring data and is more significant when the rainfall is more intense or lasts longer.

An air blast was observed at the Oujia monitoring point on June 1st, 2014, when the daily precipitation was 55.2 mm. The entire process was completed in half an hour. As shown in Fig. 7, the pressure increased rapidly and then dropped sharply. The maximum instant variation rate of groundwater–air pressure was 14 cm H_2O/min.

YR12 is by the river and was usually flooded during the rainy season. Air blasting was significant there as well. On 23 September 2013, when the daily precipitation was 46.8 mm, the groundwater–air pressure in the borehole rose from 4.8 to 27 cm H_2O within half an hour and then declined to 6.6 cm H_2O. The maximum instant variation rate was 1.7 cm H_2O/min (Fig. 8). In addition, an air blast occurred on 6 June 2014 in response to a daily precipitation of 55.2 mm. The maximum groundwater–air pressure reached 88 cmH_2O. The maximum instant variation rate was up to 9.4 cm H_2O/min (Fig. 9).

Soil Collapse

As shown in Fig. 5, of the 251 abrupt pressure change events, 36% occurred when the daily precipitation was less than 10 mm. In karst conduit systems, it is possible that groundwater–air pressure changes can be triggered by collapses of soil and rock and resultant water hammer effects.

When soil collapses occur, soils in the overburden cavity move to the underlying karst conduit system. The transported soil blocks or reduces groundwater flow through an area, which can produce abrupt groundwater–air pressure changes. Again, data at three monitoring points, YR1, Oujia,

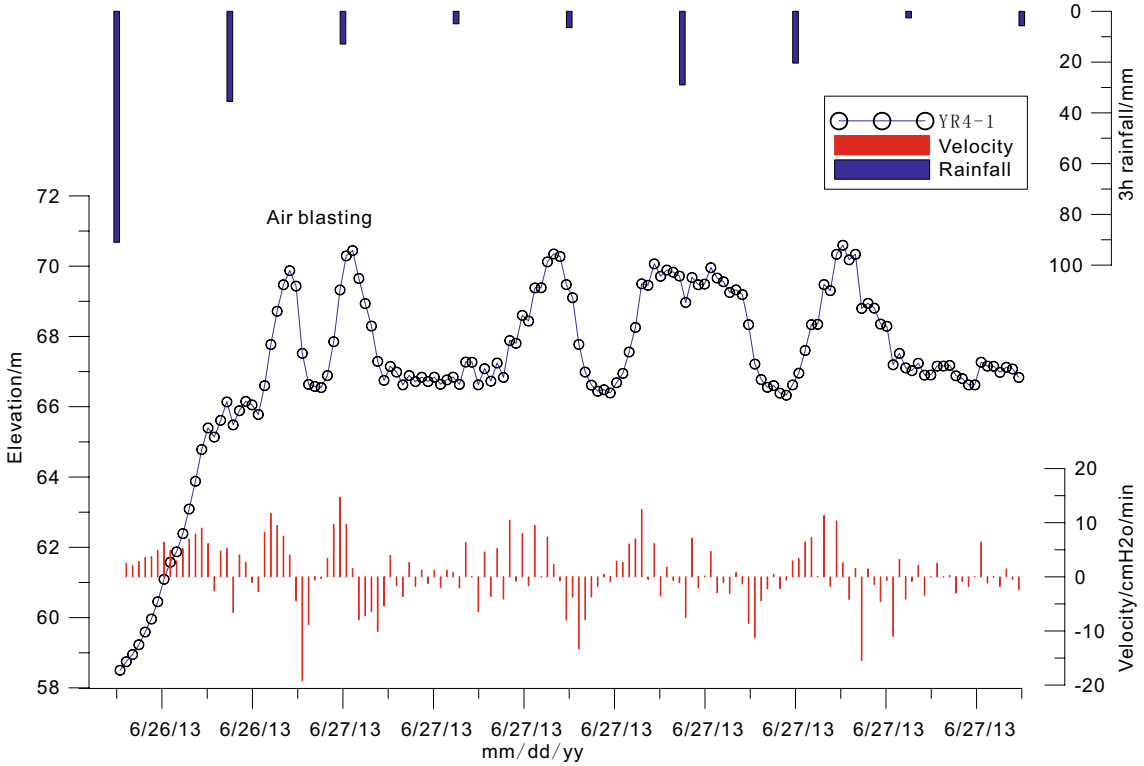

Fig. 6 Air blasting in borehole YR4-1 on 26 June 2013

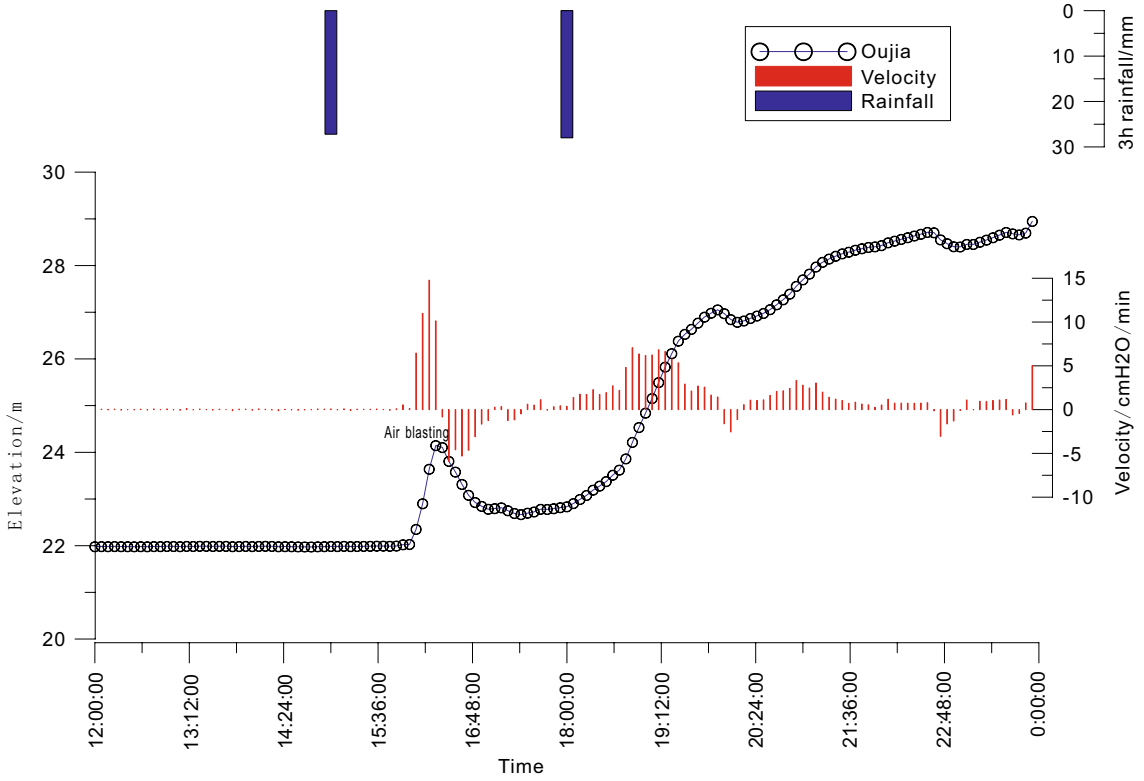

Fig. 7 Air blasting in borehole Oujia on 1 June

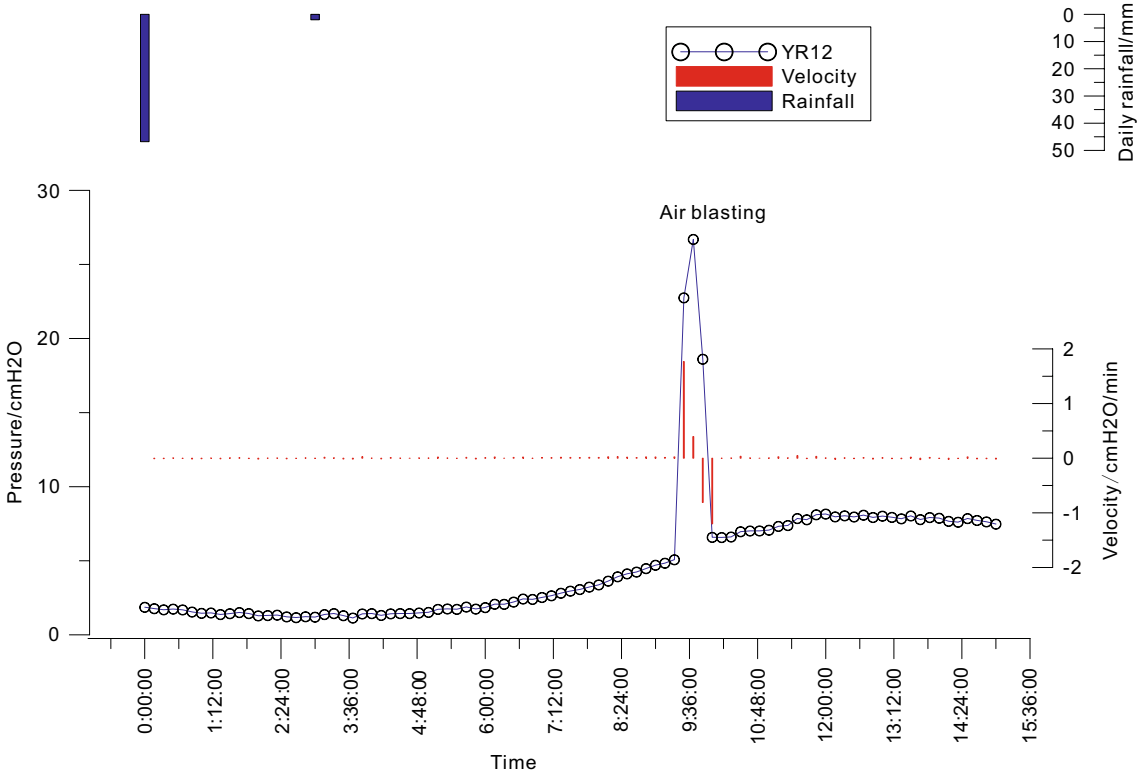

Fig. 8 Air blasting in borehole YR12 on 24 September 2013

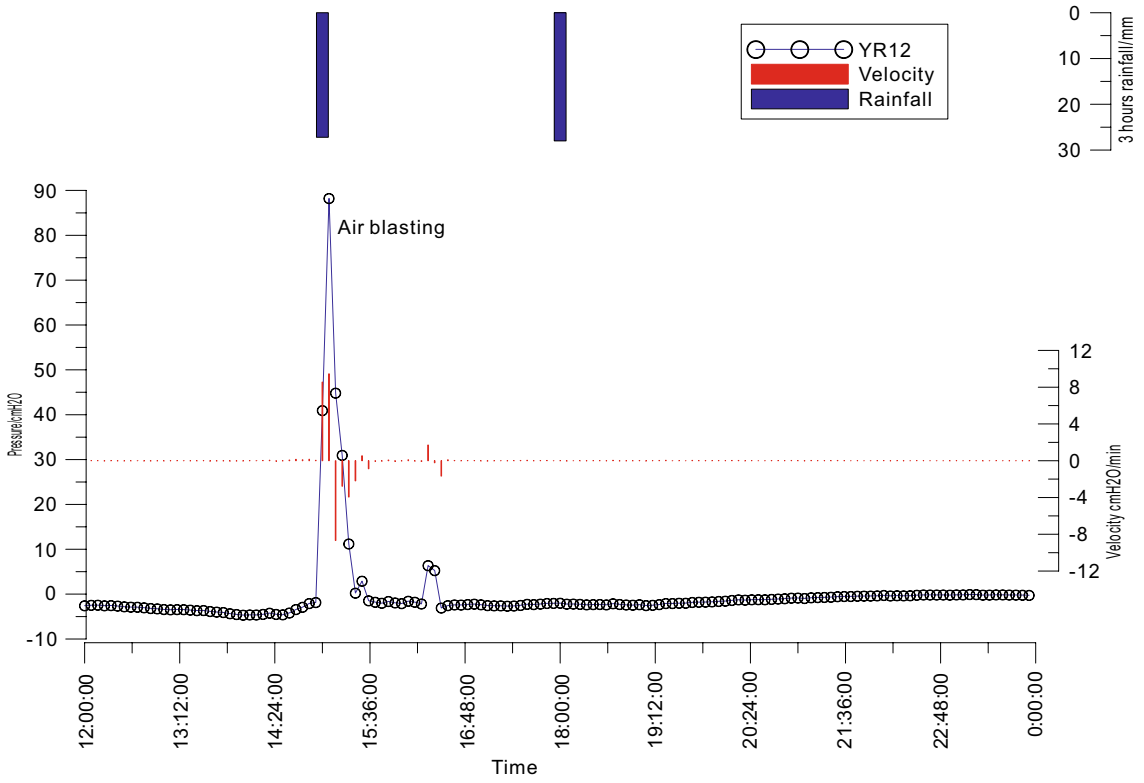

Fig. 9 Air blasting in borehole YR12 on 1 January 2014

and YR4-1, demonstrated this process. The abrupt changes of pressure caused by soil collapse are discussed below using data from YR4-1 as an example.

Monitoring point YR4-1 was installed on 13 May 2013 (Fig. 10a). On 28 May 2013, a collapse sinkhole with a diameter of 1 m occurred next to YR4-1 (Fig. 10b). Figure 11 shows the groundwater–air pressure changes. In response to a daily precipitation of 90.8 mm on 14 May 2013, the elevation of karst groundwater increased sharply by 11 m. Some air bubbles were observed bursting in the puddle. Then a significant air blast appeared on 18 May in response to rain. Though the groundwater level rose 2 m in 20 min and then dropped immediately, the general trend was rising. This means that the roof spalling of soil cavities may have caused groundwater levels to fluctuate within a range of 1 m. Finally, at 9 a.m. on 24 May, the groundwater level suddenly rose 3 m, and then the ground collapsed, forming the sinkhole.

Fig. 10 Pictures of Monitoring Point YR4-1 and collapse pit

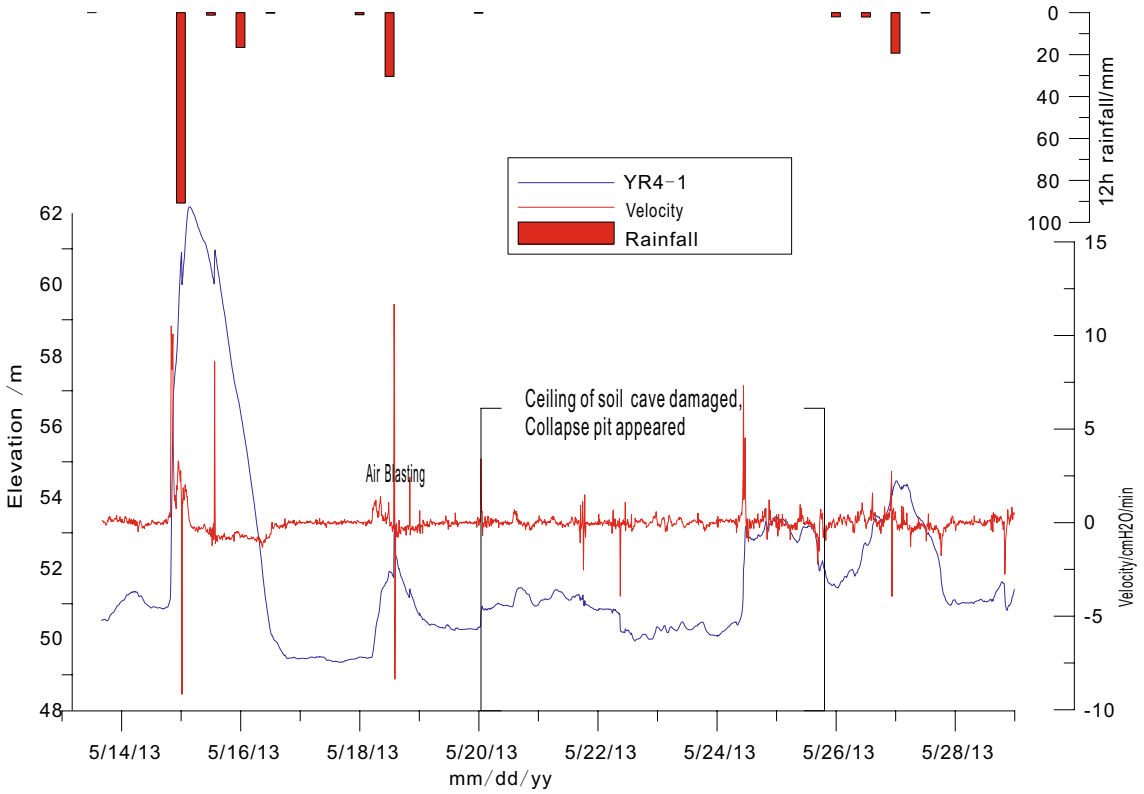

Fig. 11 Comparison of the collapse pit formation and groundwater–air pressure variation in borehole YR4-1

Significance of Abrupt Changes of Groundwater–Air Pressures in Karst Conduit Systems

Abrupt changes in groundwater–air pressures in karst conduit systems are likely an important factor triggering sinkhole formation. The monitoring data at the study area indicates that the range, rate, and frequency of pressure changes were mainly affected by rainfall, air blasts, and soil collapsing. Within the dewatering zone, where the groundwater level was below the bedrock surface, karst collapses tend to form during rainy seasons.

The key to preventing karst collapses in this area is to effectively reduce the abrupt groundwater–air pressure changes in the karst conduit system. In recent years, some measures have been taken to reduce the risk of karst collapse in this area, including installation of grouting curtains, ventilation to release pressure, and covering collapsed pits with concrete slabs. However, karst collapses still occur frequently and these measures have not been effective. According to our data analysis and investigation, four reasons contribute to their ineffectiveness:

1. The ventilation pipes were installed only to the bedrock surface where they could be easily blocked by soil erosion. Their effectiveness would be improved if the ventilation pipes were drilled into the karst conduit system.
2. The cross-sectional area of any surge chamber ventilation hole should be more than 10% of the pressurized conduit on the basis of the design code for hydropower station surge chambers (Zhang and Hou 2014), that means ventilation pipes should be at least 16 cm or more in diameter for a pressurized conduit with a diameter of 1 m. However, the diameter of the current ventilation pipes is less than 10 cm, which contributes to their ineffectiveness.
3. When the reinforced concrete slabs were placed over clay or conglomerate, soil cavities formed beneath the concrete slabs. Such cavities, when connected to a karst conduit system, could form new collapse pits at the edge of the slabs since groundwater–air pressures cannot be released immediately.
4. The abrupt groundwater–air pressure changes suggest that the groundwater flow velocity in the karst conduit system was rapid. A tracer test performed in the 1970s indicated that groundwater velocity was 39–86 m/h. So, effective grouting can be difficult.

In summary, engineering measures aiming to reduce the abrupt groundwater–air pressure changes in the karst conduit system can be improved. The ventilation pipes should be sized to release the groundwater–air pressures in the karst conduit system based on the scale of the karst space and the maximum pressure changes monitored by transducers. In addition, monitoring should continue to evaluate the effect of such improvements on sinkhole development.

Conclusions and Suggestions

Karst sinkholes have been occurring in the Dachengqiao area of the Meitanba Mine since 1984, despite the many mitigation measures that have been implemented. The sinkhole research group at the Institute of Karst Geology of China has conducted intensive investigations in this area for the last 4 years, including a geological investigation, geophysical surveys, and exploratory boreholes, to monitor the dynamic factors of the collapses. Some results are provided below:

1. There are significant abrupt groundwater–air pressure changes in the karst conduit system within the dewatering zone of the Meitanba coal mine. The maximum variation of elevation is 54.72 m and the maximum instant variation rate of groundwater–air pressures is 70.6 cm H_2O/min.
2. Using a highly precise high-frequency monitoring technique based on groundwater–air pressure variations in the karst conduit system, the triggering of karst collapses by abrupt changes in groundwater–air pressures were effectively recorded. Our analysis show that air blasts and soil collapses are major factors inducing abrupt groundwater–air pressure changes.
3. Karst collapses in this area appear to form because, during a rainstorm, the upper Quaternary deposit is saturated by surface water percolation, causing the groundwater level to rise. As a result, the air between the Quaternary deposit and karst groundwater is compressed, which causes air blasting. Air blasting damages the soil structure and forms karst soil cavities over the bedrock. In addition, the roofs of the soil cavities continue to collapse under the influence of multiple air blasts. Eventually, karst sinkholes occur on the ground surface.
4. Using ventilation boreholes should effectively reduce the influence of water hammering and air blasting in the karst conduit system. However, the ventilation borehole should be designed to reach the karst conduit system. The pipe specifications, such as size and depth, should be tailored to reflect the site-specific conditions.

Acknowledgements This study was supported by the National Natural Science Foundation of China (41472298), Special Funds of MLR for Public Welfare Projects (201211083), and the China Scholarship Council (201508450007).

References

Chen P, Chen J, Zen L (2010) The investigation report of ground collapse geohazards in Meitanba area, Ningxiang, Hunan. Hunan Province Geological Environmental Monitoring Station, Unpublished technical report **(Chinese)**

He Y, Xu C (1993) Hydrodynamic factor of karst collapse. Hydrogeol Eng 5:39–42 **(Chinese)**

Hu J, Wang Q (2007) The analysis and treatment of inrush factors in Meitanba mine. J Xiangtan Normal Univ 29(4):96–97 **(Chinese)**

Jiang X, Lei M, Zheng X, Guang Z (2016) Monitoring technology of karst collapse hazards. China Geological Press, Beijing **(Monograph ISBN 978-7-116-09685-1, Chinese)**

Little JR (1984) Relationship of modern sinkhole development to large-scale photolinear features. In: Proc. 1st multidisciplinary conf on sinkholes and the engineering and environmental impacts of Karst. Balkema, pp 189–196

Sowers GF (1996) Building on sinkholes. American Soc. of Civil Engineers Press, New York, pp 171–182

Standing J, Ghail R, Coyne D (2013) Gas generation and accumulation by aquifer drawdown and recharge in the London Basin. Q J Eng Geol Hydrogeol 46:293–302

Xiao J, Wang D, Qiu C (2008) The environmental problem and strategy of coal mining filled with karst water. J West Chin Explor Eng 3:85–87 **(Chinese)**

Zhang C, Hou J (2014) Design code for surge chamber of hydropower stations. NB/T 35021–2014, China Electric Power Press, Beijing **(Chinese)**

Zhou W, Beck BF (2008) Management and mitigation of sinkholes on karst lands: an overview of practical applications. Environ Geol 55:837–851